Available online at www.sciencedirect.com
SCIENCE DIRECT®
ELSEVIER
Journal of Magnetism and Magnetic Materials 293 (2005) 663–670
Journal of magnetism and magnetic materials
www.elsevier.com/locate/jmmm

Microrheology with modulated optical nanoprobes (MOONs)

Caleb J. Behrend[1], Jeffrey N. Anker[1], Brandon H. McNaughton, Raoul Kopelman*

University of Michigan Chemistry Department, 930 N. University, Ann Arbor, Michigan 48109-1055, USA

Available online 24 March 2005

Abstract

Metal-capping of one hemisphere of a nano or microparticle breaks the particle's optical symmetry, allowing its orientation to be tracked using fluorescence and reflection. Tracking orientation and rotation allows the torques acting on the particles be inferred. In addition to serving as rotational nanoviscometers these probes report on local Brownian, magnetic and biomechanical torques.

PACS: 83.85.Ei

Keywords: MagMOONs; Brownian motion; Microrheology; Viscosity sensor; Microscopy; Rheology; Fluorescence; Torque sensor

1. Introduction

Most fluorescent nanospheres and microspheres emit light uniformly in all directions and have spherically uniform chemical and physical properties. Coating polymer nanospheres with a metal hemisphere shell breaks this symmetry and gives the particles new optical [1,2], chemical [3–5], electrical [3,6], and other physical properties. The capped particle fluoresces, reflects, and transmits different amounts of light in different orientations, allowing its orientation to be tracked (for instance, the metal-capping blocks fluorescence from one side of fluorescing micro-sized particles making them look like the moon, Fig. 1). Tracking particle orientation reveals the torques acting on the particle, from sources including: electrical fields [3,6], magnetic fields [2], gravity [7], Brownian forces [1], biomechanical forces in macrophages [7], chemical attraction [3,8], fluid vorticity, translation/rotation coupling (rolling traction), and the opposing torque of the medium's viscous drag and elasticity [1,2,7,9]. In addition, MOONs blink when they rotate, distinguishing the MOON's optical signal from the background, and thus improving optochemical sensing measurements in samples with significant autofluorescence or electronic backgrounds [2,9–11].

*Corresponding author. Tel.: +1 734 764 7541; fax: +1 734 936 2778.
E-mail address: kopelman@umich.edu (R. Kopelman).
[1]These authors contributed equally to this article.

0304-8853/$ - see front matter © 2005 Elsevier B.V. All rights reserved.
doi:10.1016/j.jmmm.2005.02.072

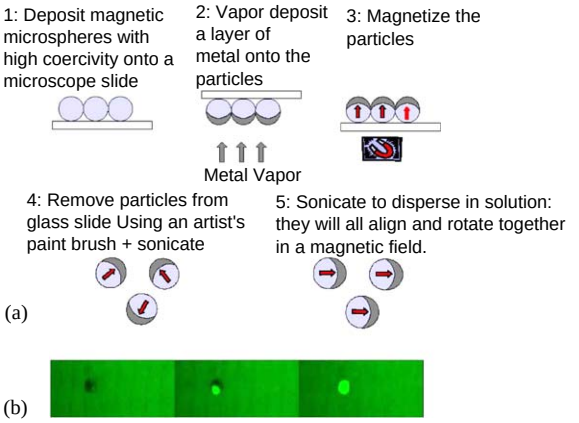

Fig. 1. (a) Preparation of metal capped modulated optical nanoprobes by vapor deposition. (b) Images of a MagMOON prepared by vacuum metallization. The fluorescent MagMOON is shown in different orientations with a constant fluorescent background.

2. Experimental section

MOONs are prepared by coating one hemisphere of a particle with a thin layer of metal, such as aluminum or gold, so that fluorescence is emitted only from the other hemisphere (moon-shaped particles) [2]. These half-coated particles also reflect light in a manner that depends strongly on orientation allowing orientation to be tracked using either reflection and/or fluorescence. A second type of MOON, aspherical MOONs, have aspherical shapes and emit different fluxes (and/or polarizations) of light from different geometric faces, due to absorption and total internal reflection within the particle [12,13]. Here, we focus mainly on metal-capped MOONs.

Prior to metal-capping, nano and microparticles can be prepared by a variety of methods including: inverse micelle polymerization [14], Stober synthesis [15], grinding larger polymer blocks into particles with a mortar and pestle [16], and ormosil formation. The particles can subsequently be modified by chemically functionalizing their surfaces, ''breading'' them with fluorescent or magnetic nanocrumbs [12,13].

A wide variety of polymer and silica nano and microspheres are commercially available. Fluorescent polystyrene microspheres 4.4 μm in diameter containing high coercivity chromium dioxide were purchased (Spherotech, Libertyville, IL). Non-magnetic polystyrene and silica spheres from 50 nm to 3 μm in diameter were purchased from Polysciences Inc.(Wharington, PA) and Estapor (France). Magnetic barium ferrite crystals 30–60 nm in diameter were a gift from Toda Kogyo Corporation.

All particles, magnetic and non-magnetic are coated with aluminum by a vacuum deposition process as illustrated in Fig. 1, and described as follows:

(i) magnetic microspheres/nanospheres are dispersed in water or ethanol solution, and a drop of solution is spread onto a glass slide and left to dry. By controlling the concentration of particles and the size of the drop, a single layer of particles can be formed. A uniform layer may also be formed using Langmuir–Blodgett techniques. The magnetic orientation of the particles is irrelevant at this stage; if they have been magnetized at all, they can be remagnetized later.

(ii) Next, the microscope slide is placed in either an aluminum vapor coater or a gold sputter coater. The aluminum is heated up in a vacuum chamber and aluminum vapor travels in a straight line (conservation of momentum) from source to target, thereby coating only one hemisphere of the particles and leaving the other hemisphere in shadow.

(iii) All the particles are now coated with metal on the same face, relative to the glass slide and to each other. The glass slide is placed in a strong magnetic field to magnetize the particles on it. The glass slide is oriented in the magnetic field so that the metal capping becomes a north-seeking pole and the uncoated side becomes a south-seeking pole. At this point the microspheres are magnetized so that their north side is uncoated.

(iv) The MagMOONs keep well on the metal-coated glass slide. They can be removed from the slide at any point using an artist's paintbrush. Sonicating the brush at 42 KHz for 30 s in aqueous solution suspends the particles.

(v) In an external magnetic field, all MagMOONs orient and align with in the direction of the field.

We have also used molecular beam deposition (MBD) to coat polymer and silica particles with cobalt. The MBD procedure allows fine uniform control over material composition and thickness, enabling tailored optical, magnetic and chemical properties on many particle types.

The preparation of Brownian MOONs is simpler than MagMOONs because neither embedded magnetic materials, nor external magnetic fields are required. Brownian MOONs require steps 1, 2, and 4, whereas steps 3 and 5, magnetization and magnetic orientation, respectively, are specific to MagMOONs. The thickness of metal capping is determined first by using a piezo-electric thickness monitor during the vacuum deposition process. It can then be verified by measuring the percentage of light transmitted through the metal coating compared to an uncoated portion of the slide assuming a skin depth of 9 nm for aluminum and 17 nm for gold for light of wavelength 589 nm [17]. The coating thickness was approximately 40 nm for the current particles. As previously reported, the metal capping of fluorescent 3.4 μm particles increases the observed intensity of emitted light by more then a factor of two [7]. This enhancement results from increased excitation path length as well as reflection towards the objective of fluorescence that would usually be emitted away from the objective.

The MagMOONs and Brownian MOONs were viewed with an Olympus IMT-II (Lake Success, NY, USA) inverted fluorescence microscope. Fluorescence spectra were acquired using an Acton Research Corp. spectrograph and a Hamamatsu HC230 CCD interfaced with an Intel Pentium computer. Images and videos of MOONs were acquired using Coolsnap ES CCD camera from Roper Scientific and a Nikon Coolpix 995 digital camera. A dichroic beam splitter from Omega Optical (Brattleboro, VT) was used to observe reflected light, while a standard Olympus blue filter cube was used for most of the fluorescence work. To modulate MagMOONs, a permanent magnet is held above the microscope stage and rotated with a stepper motor attached to the magnet. A program written in LABVIEW (National Instruments, Austin, TX) controls the stepper motor with pulses sent through the parallel port. Spectra are acquired and saved after every rotation. MagMOON orientation can also be controlled with electromagnets.

Movies of MOONs were acquired using MetaMorph software from Universal Imaging Corporation. These movies were analyzed to extract the intensity time series of blinking Brownian MOONs undergoing rotational diffusion, and magnetically rotated MagMOONs. Analysis of the timeseries was performed with Matlab V. R13 from Mathworks using vendor supplied and locally written scripts.

A range of glycerol (Spectroscopic grade, Sigma) water mixtures were prepared by percent weight using a Mettler-Toledo analytical balance. The range of glycerol concentrations in the mixture from low to high was 0–95% glycerol by mass. The solutions were stored in sealed containers to prevent absorption of water.

3. Results and discussion

MagMOONs: metal-capped MagMOONs need to have relatively high coercivity in order to orient in a magnetic field and not be remagnetized by the field. A SQUID magnetometer was used to measure the coercivity and saturation magnetization of dry powers of magnetic microspheres at room temperature. The 4.4 μm magnetic particles containing chromium dioxide shown in Figs. 2a have a coercivity of 570 ± 10 Oe. By contrast, aspherical MagMOONs orient due to shape anisotropy, and need not have a high coercivity. For instance, 1–2 μm magnetic fluorescent microspheres (Polysciences), previously used to form chain-shaped aspherical MagMOONs [13], have a coercivity of only 27 ± 2 Oe (Fig. 2b). The saturation magnetization of the particles provides a measure of the amount of magnetic material loaded into the microspheres. The Spherotech microspheres contained 18% chromium dioxide by mass, and the Polysciences contain 70% by mass.

The maximum torque induced on the metal-capped permanently magnetized MagMOONs is proportional to the product of their remnant magnetization and the magnetization of the

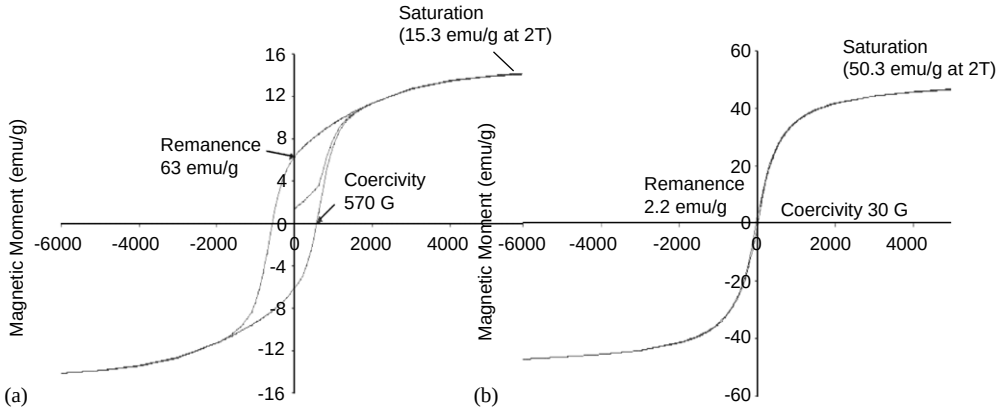

Fig. 2. The room-temperature hysteresis curve of a dry powder of: (a) 4.4 μm chromium dioxide containing polystyrene microspheres with high coercivity. (b) 1 μm iron oxide containing polystyrene particles with low coercivity.

external magnetic field. At higher driving field oscillation rates, or weaker external magnetic fields, or higher viscosities, the particles will continue to respond to the field, but will rotate with a smaller angle.

In the low Reynold's numbers regime, MagMOONs rotate at a terminal angular velocity driven by the magnetic torque. The magnetic torque and equal opposing viscous drag are described by Eqs. (1) and (2), respectively.

$$T_{\text{mag}} \approx MB \sin(\omega t - \theta), \tag{1}$$

$$T_{\text{drag}} \approx \eta V \dot{\theta}, \tag{2}$$

where M is the magnitude of the MagMOON's magnetic moment, B is the magnitude of the external magnetic field, ω is the driving frequency of the rotating external magnetic field, t is time, θ is the angle of the MagMOON moment relative to a fixed observer, η is the medium's viscosity, and V is the volume of the MagMOON.

For slow magnet rotation rates, the MagMOON follows the external magnet with a small phase lag. As the rotation rate increases, the phase lag increases. Maximum magnetic torque and MagMOON maximum velocity occurs when the external magnet is perpendicular to the MagMOON's magnetic moment. At higher driving frequencies, the MagMOON is lapped by the external magnetic field resulting in a rocking motion at the frequency of the driving field

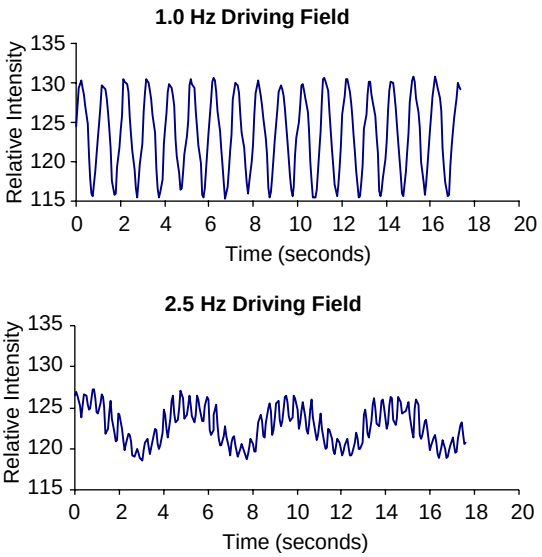

Fig. 3. (a) The fluorescence intensity time-series from a 4.4 μm MagMOON rotating at a constant angular velocity driven by an external magnet that rotates at 1.0 Hz. (b) The same MagMOON, rocking and slowly rotating, driven by the magnet rotating at 2.5 Hz.

superimposed on a slower overall rotation rate. Fig. 3 (top) shows the intensity time series from a single 4.4 μm fluorescent MagMOON in 88% glycerol (147 mPas at 20 °C, 147 times more viscous than water) driven by a 1 Hz field, and (bottom) the same particle undergoing rocking and slow rotation with a 2.5 Hz driving field.

The temporal pattern and phase lag depend on the external magnet's field strength, the particle magnetization, particle volume, particle shape, medium viscosity and elasticity, and any friction at a surface. For particles of known size and morphology, the time series reveals information about the visco-elastic properties of the medium on the size scale of the probing particle [18–22]. Conversely, if the medium is homogeneous, then the response of individual MagMOONs can be compiled into comparative statistics, giving information about the size distribution, morphology, or interactions of the MagMOONs, and, if the viscosity is known, absolute measurements can be made. Even in an inhomogeneous medium, with inhomogeneous particles, the frequency response of each particle reveals information about its local environment.

If the MagMOONs settle onto a surface, they are observed to translate as they rotate, rolling on the surface. For example, MagMOONs formed from 4.5 μm polystyrene microspheres coated with chromium dioxide (Spherotech, Libertyville, IL) and capped with an aluminum hemisphere translated approximately 0.1 radian per radian rotated when settled to a glass surface and rotating at 1 Hz. The rate of rolling depends on the particle size and shape, resulting in separation based on size, if given sufficient distance. Observing friction and slip could be used to study surface interactions, on the micro and nanoscale, as a function of rotation rate, surface properties, particle surface properties (on both metal capped and uncapped sides), shape of particle, and pressure normal to the surface. In an inhomogeneous medium, the surface interactions can occur in three dimensions, and the direction of rolling could give an insight into the local structure of the medium around the particle.

By orienting MOONs in a magnetic field, the angular dependence of the intensity of reflected or

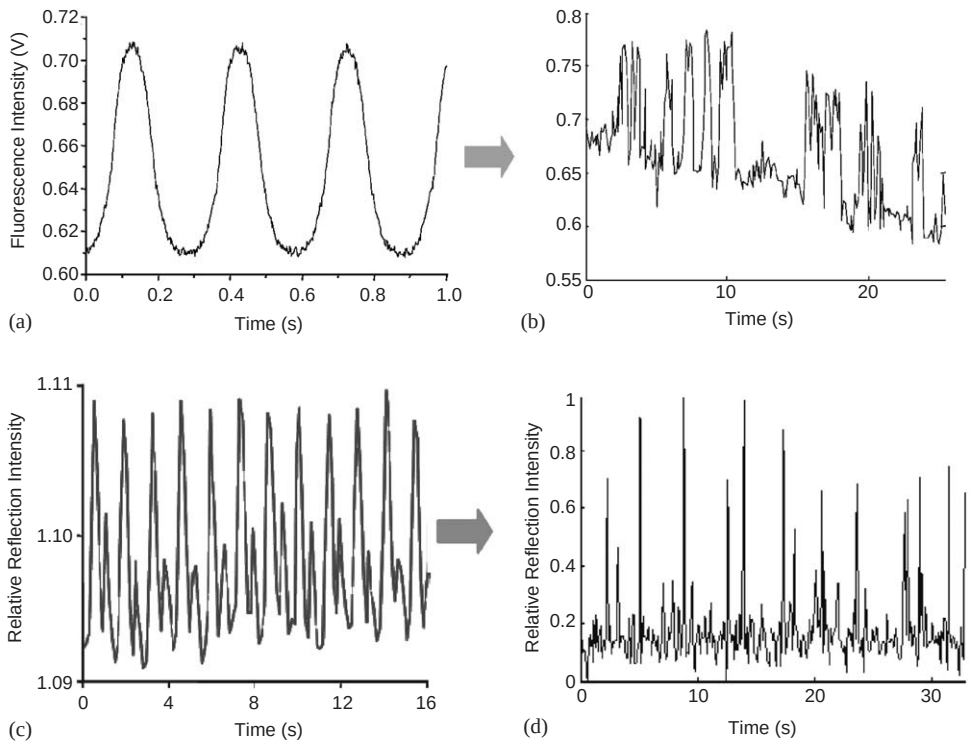

Fig. 4. (a) An ensemble of 4 μm fluorescent MagMOONs blinking at 3.3 Hz. (b) A single 2 μm Brownian MOON in the absence of magnetic fields. (c) Reflection intensity time-series for a single 4.4 μm aluminum-coated MagMOON (d) Reflection intensity time-series for a single 150 nm aluminum-coated Brownian MOON.

emitted light can be observed. For fluorescent and reflecting MagMOONs this time series is periodic (Figs. 4a and c). For fluorescence the observed intensity waveform has a fundamental frequency, as well as a first harmonic of approximately $\frac{1}{3}$ the magnitude, and some weaker higher order harmonics [2]. The pattern is more complicated in the case of reflection, showing blinking occurring twice per revolution rather than once, with alternating high and low intensities as shown in Fig. 4(c).

Brownian MOONs: In the absence of external rotating magnetic fields, or for MOONs containing no magnetic material, the only surviving rotational motion of the MOONs is due to Brownian motion (rotation), as shown in Fig. 4(b) with fluorescence and Fig. 4(d) with reflection. Fig. 5 shows images of a number of Brownian MOONs, each rotating independently. Figs. 5(a) and (b) show 3.4 μm Brownian MOONs viewed under fluorescence, while Figs. 5(c) and (d) show diffraction limited 50 nm Brownian MOONs, viewed under reflection.

This time series of intensity fluctuations contains information about the local rheology as well as information about the particle shape, size, and its interaction with its environment. Torques experienced by the particle and revealed by the

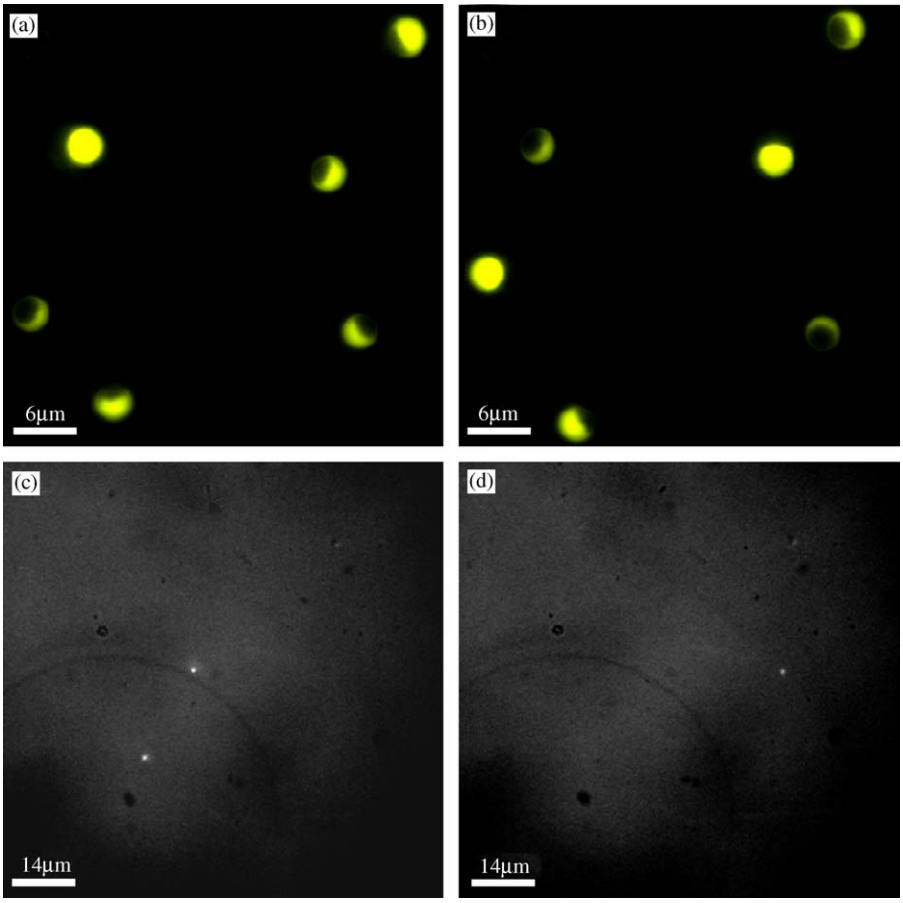

Fig. 5. The top two images, (a) and (b), show fluorescence from six different 3.4 μm aluminum-capped Brownian MOONs individually rotating through the phases of the moon at two different times. The bottom two images, (c) and (d), show reflection from diffraction limited 50 nm aluminum-capped Brownian MOONs and aggregates flickering on an off in a solution of 88% glycerol at two different times.

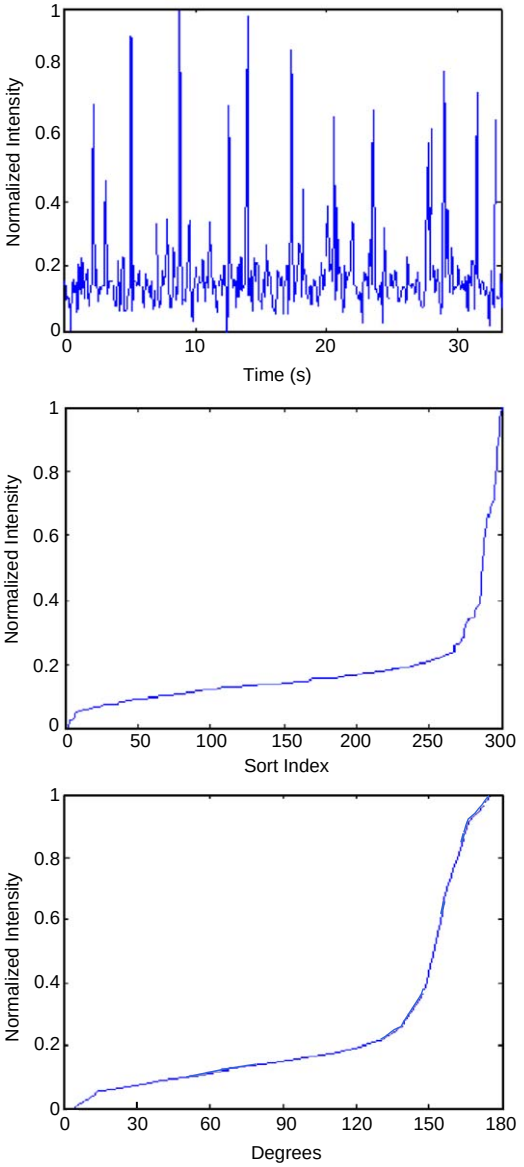

Fig. 6. (a) Intensity time series for a 150 nm reflecting moon undergoing rotational diffusion. (b) The sorted intensity values for the same 150 nm reflecting particle. (c) Calculated angle intensity function.

blinking pattern include: viscous drag, elastic forces, binding interactions, gravitational torques, vorticity in fluid flow, and biomechanical forces.

The top panel of Fig. 6 shows the intensity time series for a single 150 nm Brownian MOON observed in reflection. These MOONs do flash "on" for brief periods, and spend most of the time in orientations closer to "off." A sort of the intensities in the series, the middle panel of Fig. 6, shows that approximately 270 of 300 intensities are relatively low. Assuming that all angular orientation states are visited with equal probability, and accounting for the differences in density of states at each azimuthal angle [7], the bottom panel of Fig. 6 shows the angle intensity function for the 150 nm particle. Included is the assumption that the intensity increases monotonically with angle, which may not be valid for reflecting particles, because of their reflection from both faces, as shown in Fig. 5c. This plot indicates that the intensity is weak for particle angles smaller than 140° and increases rapidly for angles greater than 140°. Longer acquisition times, and shorter exposure times, give a better defined characterization. For 2 μm fluorescent Brownian MOONs the profile is more gradual [7].

In the prepared glycerol water solutions, viscous drag is the only significant torque damping the Brownian MOON fluctuations. We use the autocorrelation function of the intensity time-series to provide a measure of the angular diffusion rate. In addition to viscosity, variation in particle size, angular intensity function, and particle environment also affect the autocorrelation function.

There are advantages to using reflection over fluorescence. Smaller particles, such as 50 nm aluminum-coated particles and 60 nm barium ferrite crystals, give a strong optical signal, compared to fluorescent particles of similar size. Also, the probes are photostable and can be used with high intensity light sources, over a broad range of wavelengths.

This new approach will enable one to obtain high resolution images of viscoselastic properties of local environments. It also allows characterization of the drag on a MOON that is induced by binding, such as the binding of 50 nm viruses to 100 nm Brownian MOONs. Some of these applications require control over the binding location, relative to the capping material, because the location of the binding affects the observed rotation rate. Control could be achieved by chemically binding or physically pressing

(''breading'') smaller particles into large particles, before metal capping [7,12,13,18].

4. Conclusions

Observing the response of MagMOONs to external fields, and analyzing the angular rotation of Brownian MOONs, provides a new tool for studying viscous drag and torques on the scale of microns to tens of nanometers. Also, using reflection, rather than fluorescence, from the MOONs allows for the use of smaller particles, thus extending the accessible ranges of size and time for this technique. Applying the concept of controlled optical, chemical, and magnetic symmetry to micro or nanoparticles, results in novel tools and techniques for exploring the physical and chemical world. Nanoviscometers [10,18–22], nanothermometers [23], nanobarometers, and nanochemical sensors [24] are examples of probes that can be produced using these principles.

Acknowledgment

The authors gratefully acknowledge support from DARPA F49620-03-1-0297.

References

[1] C.J. Behrend, J.N. Anker, R. Kopelman, Appl. Phys. Lett. 84 (2004) 154.
[2] J.N. Anker, R. Kopelman, Appl. Phys. Lett. 82 (2003) 1102.
[3] H. Takei, N. Shimizu, Langmuir 13 (1997) 1865.
[4] L.A. Cameron, M.J. Footer, et al., P. Nat. Acad. Sci. USA 96 (1999) 4908.
[5] J.R. Link, M.J. Sailor, P. Nat. Acad. Sci. USA 100 (2003) 10607.
[6] J.M. Crowley, N.K. Sheridon, L. Romano, J. Electrostat. 55 (2002) 247.
[7] C.J. Behrend, J.N. Anker, et al., J. Phys. Chem. 108 (2004) 10408.
[8] J. Choi, Y.H. Zhao, D.Y. Zhang, et al., Nano Lett. 3 (2003) 995.
[9] B.H. McNaughton, J.N. Anker, R. Kopelman. J. Magn. Magn. Mater., this issue.
[10] J.N. Anker, C.J. Behrend, et al., Mat. Res. Soc. Symp. Proc. 790 (2004) 4.4.1-12.
[11] T.G. Roberts, J.N. Anker, R. Kopelman. J. Magn. Magn. Mater., this issue.
[12] J.N. Anker, T.D. Horvath, R. Kopelman, Eur. Cells. Mat. 3 (2002) 95.
[13] J.N. Anker, C. Behrend, R. Kopelman, J. Appl. Phys. 93 (2003) 6698.
[14] H.A. Clark, M. Hoyer, M.A. Philbert, et al., Anal. Chem. 71 (1999) 4831.
[15] H. Xu, F. Yan, E.E. Monson, et al., J. Biomed. Mater. Res. A 66A (2003) 870.
[16] K. Sasaki, Z.Y. Shi, R. Kopelman, et al., Chem. Lett. (1996) 141.
[17] M. Born, E. Wolf, Principles of Optics, sixth Ed., Cambridge University Press, New York, NY, 1980 (Chapter 13).
[18] V. Santhanam, R.P. Andres, Nano Lett. 4 (2004) 41.
[19] F.C. Mackintosh, C.F. Schmidt, Curr. Opin. Colloid In. 4 (1999) 300.
[20] Y. Nicolas, M. Paques, A. Knaebel, et al., Rev. Sci. Instrum. 74 (2003) 3838.
[21] V. Breedveld, D.J. Pine, J. Mater. Sci. 38 (2003) 4461.
[22] K.J. Van Vliet, G. Bao, S. Suresh, Acta Mater. 51 (2003) 5881.
[23] O. Zohar, M. Ikeda, H. Shinagawa, et al., Biophys. J. 74 (1998) 82.
[24] E. Monson, M. Brasuel, M.A. Philbert, et al., in: T. Vo-Dinh (Ed.), Biomedical Photonics Handbook, CRC Press, Boca Raton, FL, 2003.